Journal of Molecular Structure 969 (2010) 25–32

Contents lists available at ScienceDirect

Journal of Molecular Structure

journal homepage: www.elsevier.com/locate/molstruc

Synthesis, X-ray and spectroscopic analysis of some pyridine derivatives

Mario Cetina [a,*], Marina Tranfić [b], Igor Sviben [b], Marijana Jukić [b,*]

[a] Department of Applied Chemistry, Faculty of Textile Technology, University of Zagreb, Prilaz baruna Filipovića 28a, HR-10000 Zagreb, Croatia
[b] Department of Chemistry and Biochemistry, Faculty of Food Technology and Biotechnology, University of Zagreb, Pierottijeva 6, HR-10000 Zagreb, Croatia

ARTICLE INFO

Article history:
Received 11 December 2009
Received in revised form 18 January 2010
Accepted 18 January 2010
Available online 25 January 2010

Keywords:
Substituted 2-pyridones
X-Ray structure analysis
IR
NMR and UV–vis spectroscopy

ABSTRACT

Three pyridine derivatives, 4-(methoxymethyl)-6-methyl-2-oxo-1,2-dihydropyridine-3-carbonitrile (**1**), 4-(methoxymethyl)-6-methyl-5-nitro-2-oxo-1,2-dihydropyridine-3-carbonitrile (**2**) and 4-(methoxymethyl)-1,6-dimethyl-2-oxo-1,2-dihydropyridine-3-carbonitrile (**3**) have been synthesized, and their structural features have been studied by IR and electronic spectroscopy. The optical properties were investigated by UV–vis absorption and fluorescence spectroscopy. Fluorescence spectra of compounds have been recorded in two protic and two aprotic solvents in the range of 200–600 nm. The effects of substituents on the emission spectra of these compounds are interpreted. The structures of compounds **2** and **3** were also confirmed by single crystal X-ray diffraction method.

© 2010 Elsevier B.V. All rights reserved.

1. Introduction

Among many naturally occurring and synthetic compounds are these with 2-pyridone skeleton which possess interesting pharmacological properties. Pyridone derivatives are reported to possess many biological activities [1] such as antibacterial [2], antifungal [3], antiviral [4] and antitumor [5–7]. Pyridone ring substituents influence on the biological activity type. Thus, the presence of nitro group has been crucial for developing antifungal efficacy of such compounds [8]. Some 2-pyridone derivatives are also of considerable biological importance as cardiotonic agents such as Milrinone (2-oxo-1,2-dihydropyridine-3-carbonitrile) [9–11] for the treatment of heart failure and as potential HIV-1 specific transcriptase inhibitors [12–15]. *N*-alkylated 2-pyridones are important intermediates in the synthesis of polycyclic compounds of biological significance as illustrated by the recent synthetic approaches toward the camptothecin family of antitumor agents [16,7].

The different ligands of 2-pyridone (or 2-hydroxypyridine) and its derivatives have been shown to form a large number of complexes with various metals, affording mononuclear, dinuclear and polynuclear compounds, as extensively investigated by Cotton et al. [17]. These ligands exhibit a variety of bonding modes and, in particular, have played an important role in the understanding of metal–metal multiple bonds. Recently, molecular magnetism and redox activities of transition metal complexes have attracted attention [18–20].

The prominent role played by pyridones and related compounds as privileged structures in many natural products and bioactive compounds, led us to consider the extension of our studies to the 2-pyridone nucleus. The present work has been undertaken as a part of our systematic research on the synthesis and analysis of heterocyclic molecules [21–23], and continues our investigation of structures these bioactive compounds and their metal complexes. The goal of this work was to carry out further characterization of various derivatives of pyridones. Particularly, we wanted to determine how the position and number of substituents modulate their spectroscopic properties.

2. Experimental

2.1. General

All reactions were performed with commercially available reagents and they were used without further purification. Solvents were dried by standard methods and stored over molecular sieves (4 A). All reactions were monitored by thin-layer chromatography (TLC) carried out on Merck, DC-Alufolien Kieselgel 60 F254, and detection of the components was made by short and long UV light.

Products were purified by preparative thin-layer chromatography on silica gel (Merck, Kieselgel 60 HF254) using the mixtures CH_2Cl_2:EtOAc and/or by recrystallization from (aqueous) EtOH. The solvents were of spectroscopic grade.

The chemical structure and the purity of the compounds were confirmed by melting points, FTIR, ^1H and ^{13}C NMR spectra. Ultraviolet absorption spectra of synthesized compounds have been recorded in the region 200–600 nm in four different solvents and the effects of substituents and solvents was investigated on the absorption spectra.

* Corresponding authors. Tel.: +385 1 3712 590; fax: +385 1 3712 599 (M; Cetina); Tel.: +385 1 4605 282; fax: +385 1 4836 083 (M. Jukić).
E-mail addresses: mario.cetina@ttf.hr (M. Cetina), mjukic@pbf.hr (M. Jukić).

0022-2860/$ - see front matter © 2010 Elsevier B.V. All rights reserved.
doi:10.1016/j.molstruc.2010.01.038

The melting points were determined using an electrothermal Buechi apparatus and are not corrected. The IR spectra were recorded for KBr pellets or CH_2Cl_2 solutions with a Bomem MB 100 mid FTIR spectrophotometer. The ^1H and ^{13}C NMR spectra were recorded on a Bruker Avance 300 or Bruker Avance 600 MHz spectrometer in DMSO-d_6 solution with Me_4Si as internal standard. Ultraviolet visible (UV–vis) absorption spectra and fluorescence spectra were recorded using an Ocean optics USB 4000 spectrophotometer and a Varian Cary fluorescence spectrophotometer at wavelength of maximum absorption (λ_{max}) in water, ethanol, tetrahydrofuran and dichloroethane. The UV–vis spectra were obtained at room temperature and fluorescence spectra at 25 ± 0.1 °C, both using 1 cm optical path-length quartz cells.

2.2. Synthesis

The synthesis of the compounds was performed according to the following scheme 1.

2.2.1. 4-(Methoxymethyl)-6-methyl-2-oxo-1,2-dihydropyridine-3-carbonitrile (**1**)

Yield 81%, m.p. 233–236 °C; elemental analysis, calculated for $C_9H_{10}N_2O_2$ (178.189); % C 60.67; % H 5.66; % N 15.72. Found: % C 60.71; % H 5.58; % N 15.67; IR (KBr): ν 3302 (N–H), 3099 (aromatic C–H), 3003, 2829 (aliphatic C—H), 2214 (C≡N), 1656 (C = O), 1626 (C = C), 1584 (N—H), 1194 (CONH–), 573 (CONH–) cm^{-1}; ^1H-NMR (DMSO-d_6) 12.49 (s, 1H, N—H), 6.28 (1H, s, C–5), 4.43 (2H, s, CH_2O), 3.39 (3H, m, OCH_3), 2.52 (3H, s, CH_3, C–6) ppm; ^{13}C-NMR, APT (DMSO-d_6) δ 160.84 (C = O), 160.19 (C–4), 152.65 (C–3), 114.99 (C–6), 103.71 (CH, C–5), 96.38 (C≡N), 70.52 (CH_2O), 58.36 (OCH_3), 19.13 (CH_3) ppm.

2.2.2. 4-(Methoxymethyl)-6-methyl-5-nitro-2-oxo-1,2-dihydropyridine-3-carbonitrile (**2**)

Yield 78%, m.p. 108–109 °C; elemental analysis, calculated for $C_9H_9N_3O_4$ (223.1862); % C 48.43; % H 4.06; % N 18.83. Found: % C 48.36; % H 4.18; % N 18.81; IR (KBr): ν 3312 (N—H), 3072 (aromatic C—H), 3004, 2839 (aliphatic C—H), 2225 (C≡N), 1658 (C = O), 1614 (C = C), 1578 (N—H), 1367 (C–NO_2) 1183 (CONH–), 568 (CONH–) cm^{-1}; ^1H-NMR (DMSO-d_6) 13.27 (s, 1H, N-H), 4.58 (2H, s, CH_2O), 3.35 (3H, m, OCH_3), 2.49 (3H, s, CH_3, C–6) ppm; ^{13}C-NMR, APT (DMSO-d_6) δ 159.41 (C = O), 151.82 (C–5), 151.26 (C–4), 132.21 (C–3), 114.21 (C–6), 101.56 (C≡N), 69.73 (CH_2O), 59.26 (OCH_3), 17.70 (CH_3) ppm.

2.2.3. 4-(Methoxymethyl)-1,6-dimethyl-2-oxo-1,2-dihydropyridine-3-carbonitrile (**3**)

Yield 89%, m.p. 206–208 °C; elemental analysis, calculated for $C_{10}H_{12}N_2O_2$ (192.216); % C 62.49; % H 6.29; % N 14.57. Found: % C 62.38; % H 6.31; % N 14.46; IR (KBr): ν 3662 (N–CH_3), 3091 (aromatic C–H), 2996, 2819 (aliphatic C—H), 2222 (C≡N), 1656 (C = O) cm^{-1}; ^1H-NMR (DMSO-d_6) δ 6.42 (1H, s, C–5), 4.43 (2H, s, CH_2O), 3.47 (3H, s, N–CH_3), 3.36 (3H, m, OCH_3), 2.47 (3H, s, CH_3, C–6) ppm; ^{13}C-NMR, APT (DMSO-d_6) δ 160.93 (C = O), 157.99 (C–6), 155.16 (C–4), 115.60 (C–3), 105.44 (CH,C–5), 96.25 (C≡N), 70.80 (CH_2O), 58.89 (OCH_3), 31.83 (N–CH_3), 21.56 (CH_3) ppm.

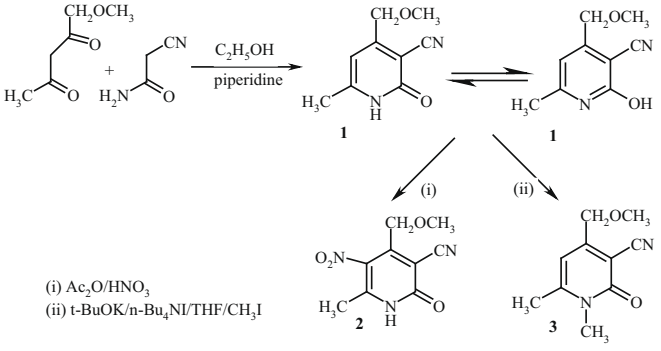

Scheme 1. Synthesis of the pyridine derivatives **1**, **2** and **3**.

2.3. Crystal structure determination

Single crystal of **2** suitable for X-ray single crystal analysis was obtained at room temperature by partial evaporation from methanol solution. Single crystal of **3a** was obtained applying the same method from ethanol solution. Its triclinic polymorph **3b** was obtained by recrystallization from acetone/water mixture (2:1). The intensities were collected at 295 K on a Oxford Diffraction × calibur2 diffractometer using graphite-monochromated Mo*K*α radiation (λ = 0.71073 Å). *CrysAlis* [24] programs were used for data collection and reduction. The intensities were corrected for Lorentz and polarization effects, and for extinction for **3a**. The crystal structures were solved by direct methods [25]. All non-hydrogen atoms were refined anisotropically by full-matrix least-squares calculations based on F^2 [25]. The hydrogen atom of the N1 atom in **2** was found in a difference Fourier map and its coordinates and isotropic thermal parameter have been refined freely. All other hydrogen atoms in **2**, and all hydrogen atoms in **3a** and **3b** were included in calculated positions as riding atoms, with *SHELXL97* [24] defaults. The O3 and O4 atoms of nitro group, as well as O2 and C9 atoms of methoxy group in **2** are statistically disordered over two sites, with the occupancy ratio of 57.8(4)% and 42.2(4)%, respectively. The disordered atoms were modelled with the help of similarity restraints for anisotropic displacement parameters. Details of crystal data, data collection and refinement parameters are given in Table 1. *PLATON* [26] program was used for structure analysis and drawings preparation. CCDC 757,132–757,134 contain the supplementary crystallographic data for this paper. These data can be obtained free of charge from The Cambridge Crystallographic Data Centre via www.ccdc.cam.ac.uk/data_request/cif.

3. Results and discussion

Compound **1** (4-(methoxymethyl)-6-methyl-2-oxo-1,2-dihydropyridine-3-carbonitrile) was synthesised by starting from the methyl acetoacetic ester in ethanol followed by condensation with cyanoacetamide using piperidine as catalyst, using previously described synthetic methods [27] with minor modifications. The pyridone **1** was converted to pyridone **2** (4-(methoxymethyl)-6-methyl-5-nitro-2-oxo-1,2-dihydropyridine-3-carbonitrile) according to modified Harris–Folkers [27] procedures in terms of isolation techniques as well as purification and identification of the products. Compound **3** was done with *N*-alkylation's of compound **1** by slight adjustment of the Conreaux et al. [28] procedure. Selective *N*-methylation of 4-(methoxymethyl)-6-methyl-2-oxo-1,2-dihydropyridine-3-carbonitrile (**1**) has been achieved with methyl iodide under mild conditions with tetrabutylammonium iodide and potassium tert-butoxide being employed as the catalyst, respectively. We found that better yields were obtained when the reaction was performed in THF solution at about 50–55 °C for 2 h (instead stirred overnight at room temperature). Minor modifications were also made in isolation and purification techniques (TLC-purification) of the product. *N*-methyl pyridone **3** was synthesized as reference compound for spectroscopic studies because it cannot tautomerize and the possible tautomeric hydroxypyridine forms of compounds **1** and **2** could be than easily identified by ^1H NMR and UV spectroscopy.

Table 1
X-ray crystallographic data for **2**, **3a** and **3b.**

Compound	**2**	**3a**	**3b**
Formula	$C_9H_9N_3O_4$	$C_{10}H_{12}N_2O_2$	$C_{10}H_{12}N_2O_2$
Formula weight	223.19	192.22	192.22
Crystal size [mm]	0.13 × 0.48 × 0.71 mm	0.11 × 0.65 × 0.70	0.19 × 0.26 × 0.65
Crystal colour, shape	–	Colourless, prismatic	–
Crystal system	monoclinic	orthorhombic	triclinic
Space group	$P\,2_1/c$	$P\,b\,c\,a$	$P\bar{1}$
Unit cell dimensions			
a [Å]	13.1791(5)	8.2775(4)	7.1765(2)
b [Å]	7.0434(2)	10.6127(7)	13.2533(4)
c [Å]	12.5685(5)	22.0187(13)	16.3305(6)
α [°]	90.00	90.00	100.543(3)
β [°]	116.104(5)	90.00	101.158(3)
γ [°]	90.00	90.00	93.935(2)
V [Å^3]	1047.67(6)	1934.3(2)	1489.40(8)
Z	4	8	6
$D_{calc.}$ [g cm^{-3}]	1.415	1.320	1.286
Absorption coefficient μ [mm^{-1}]	0.114	0.094	0.091
$F(000)$	464	816	612
Scan mode	ω	ω	ω and φ
θ range [°]	4.16–28.00	3.95–27.99	3.89–28.00
Index ranges	$-16 \leqslant h \leqslant 17$ $-9 \leqslant k \leqslant 9$ $-16 \leqslant l \leqslant 16$	$-10 \leqslant h \leqslant 10$ $-14 \leqslant k \leqslant 13$ $-28 \leqslant l \leqslant 29$	$-9 \leqslant h \leqslant 9$ $-17 \leqslant k \leqslant 17$ $-21 \leqslant l \leqslant 21$
Collected reflections no.	12,334	18,350	42,545
Independent reflections No. / $R_{int.}$	2519 / 0.0275	2314 / 0.0399	7179 / 0.0366
Reflections no. $I \geqslant 2\sigma(I)$	1460	1683	3789
Data / restraints / parameters	2519 / 50 / 187	2314 / 0 / 131	7179 / 0 / 388
Goodness-of-fit on F^2, S	0.983	1.082	1.049
R [$I \geqslant 2\sigma(I)$] / R [all data]	0.0466 / 0.0772	0.0518 / 0.0703	0.0501 / 0.1085
wR [$I \geqslant 2\sigma(I)$] / wR [all data]	0.1344 / 0.1422	0.1463 / 0.1692	0.1399 / 0.1664
Max./min. el. density [e Å^{-3}]	0.188 / −0.231	0.274 / −0.229	0.161 / −0.223

3.1. X-ray crystal structure analysis

4-(Methoxymethyl)-1,6-dimethyl-2-oxo-1,2-dihydropyridine-3-carbonitrile (**3**) crystallized in orthorhombic space group $P\,b\,c\,a$ (**3a**) and triclinic space group $P\bar{1}$ (**3b**) with three independent molecules in the asymmetric unit (Figs. 1 and 2). The six-membered heterocycle ring has a well defined diene-like structure; the C3–C4 and C5—C6 bonds are shorter than bonds C2—C3 and C4—C5. In order to compare these two structures, and structure of 4-(methoxymethyl)-6-methyl-5-nitro-2-oxo-1,2-dihydropyridine-3-carbonitrile (**2**) with closely related ones we searched Cambridge Structural Database [29] for 6-methyl-2-oxo-1,2-dihydropyridine-3-carbonitrile, in which carbon atom substituent is bonded to C4 atom of the pyridine ring (error-free and disorder-free structures with $R < 0.075$). An analysis reveals that equivalent bond lengths in **2**, **3a** and **3b** are in a good agreement, as well as with those in similar structures [30–35]. The exceptions are N1—C2 and N1—C6 bond lengths which are slightly shorter (ca. 0.02–0.03 Å) in **2** (Fig. 3) and closely related structures [30,32,33]. In these structures, hydrogen atom is bonded to the 2-pyridone ring nitrogen atom, whereas in others, it is substituted with methyl group (**3a**, **3b**) or some other substituent [31,34,35].

The atoms of nitro (O3, O4) and methoxy group (C9, O2) in **2** are statistically disordered, so defining two different orientations of these groups with respect to the 2-pyridone ring. The nitro group is twisted away from the 2-pyridone ring by 67.8(5)° and 63.7(5)° for major and minor components, respectively.

Three independent molecules of **3b** differ in the conformation of the methoxy group with respect to the 2-pyridone ring. In the molecules designated as B and C, the conformation defined by the C3C4C8O2 and C9O2C8C4 torsion angles is antiperiplanar (C3B(C4B(C8B(O2B = 175.47(16)°; C3C(C4C(C8C(O2C = 174.20(15)°; C9B(O2B(C8B(C4B = 175.62(18)°; C9C(O2C(C8C(C4C = 177.8(2)°. Same conformation has methoxy group in 3a (C3(C4(C8(O2 = 177.30(12)°; C9(O2(C8(C4 = 178.49(12)°, so enabling intramolecular hydrogen bond formation. Thus, C5···O2 intramolecular hydrogen bond (Table 2) in 3a and B and C independent molecules of 3b generates five-membered ring which can be described by graph-set notation as S(5) [36]. On the contrary, conformation of methoxy group in A molecule of **3b** is synclinal (Fig. 2), with the C3C4C8O2 and C9O2C8C4 torsion angles of 49.1(2)° and 74.4(2)°, respectively.

The molecules of **3a** are mutually parallel and disposed in a herringbone fashion. They are held together only by van der Waals forces (Fig. 4), what is the first such example as molecules of

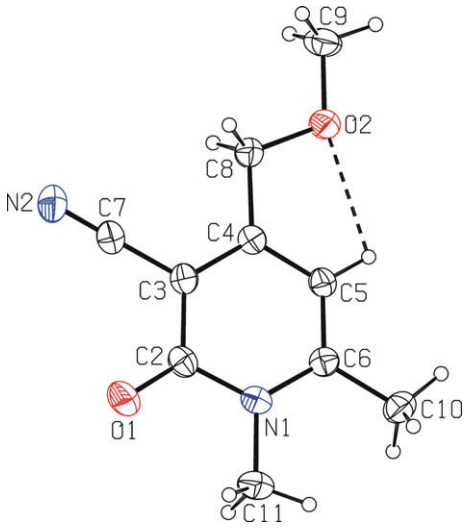

Fig. 1. A molecular structure of **3a**, with the atom-numbering scheme. Displacement ellipsoids for non-hydrogen atoms are drawn at the 30% probability level. The intramolecular hydrogen bond is shown dashed.

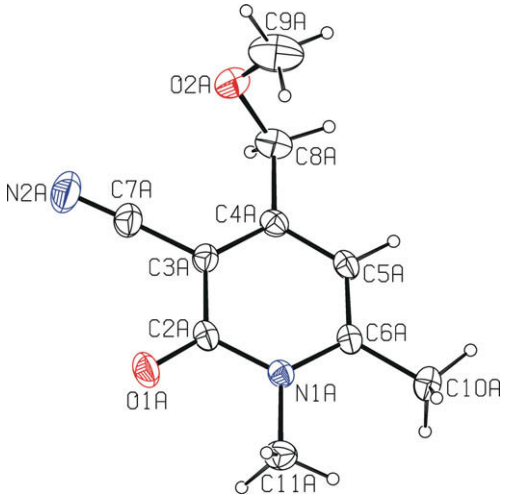

Fig. 2. A molecular structure of **3b**, with the atom-numbering scheme. For clarity, only one of three independent molecules in the asymmetric unit is shown. Displacement ellipsoids for non-hydrogen atoms are drawn at the 20% probability level.

closely related structures [30–35] are linked by at least one hydrogen bond.

The supramolecular structure of **3b** contains two intermolecular hydrogen bonds that link only A independent molecules (Table 2; Fig. 5). Thus, C5A···O1A hydrogen bond self-assembles A molecules into C(6) chains, and C11A···O1A hydrogen bond joins two A molecules into centrosymmetric dimer of $R_2^2(10)$ type. The combination of these two motifs forms tetramers through $R_4^2(14)$ rings which are further linked by C5A···O1A hydrogen bond into infinite chain of tetramers.

The N1···O1 hydrogen bond in **2** generates characteristic supramolecular synthon, centrosymmetric $R_2^2(8)$ dimer (Fig. 6). Hydrogen-bonded dimers are parallel to each other, but disposed in two almost perpendicular opposite directions.

3.2. Spectral analysis

3.2.1. UV–vis and fluorescence spectra

In this work, ultraviolet spectra of compounds **1**–**3** have been recorded in two protic and two aprotic solvents in the range of

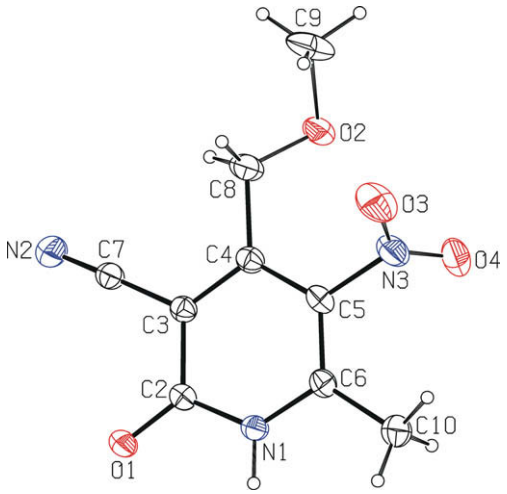

Fig. 3. A molecular structure of **2**, with the atom-numbering scheme. For clarity, only major component of disordered atoms is shown. Displacement ellipsoids for non-hydrogen atoms are drawn at the 20% probability level.

Table 2
Hydrogen-bonding geometry for **2**, **3a**, and **3b.**

	D–H···A	D–H (Å)	H···A (Å)	D···A (Å)	D–H···A (°)	Symmetry codes
2	N1–H···O1	0.91(2)	1.86(2)	2.7667(17)	179(3)	$-x, -y, -z$
3a	C5–H···O2	0.93	2.37	2.7218(17)	102	
3b	C5B–H···O2B	0.93	2.38	2.723(2)	102	
	C5C–H···O2C	0.93	2.39	2.732(2)	102	
	C11B–H···O1B	0.96	2.27	2.669(3)	104	
	C5A–H···O1A	0.93	2.29	3.197(2)	166	$-1+x, y, z$
	C11A–H···O1A	0.96	2.57	3.524(3)	175	$2-x, 1-y, 1-z$

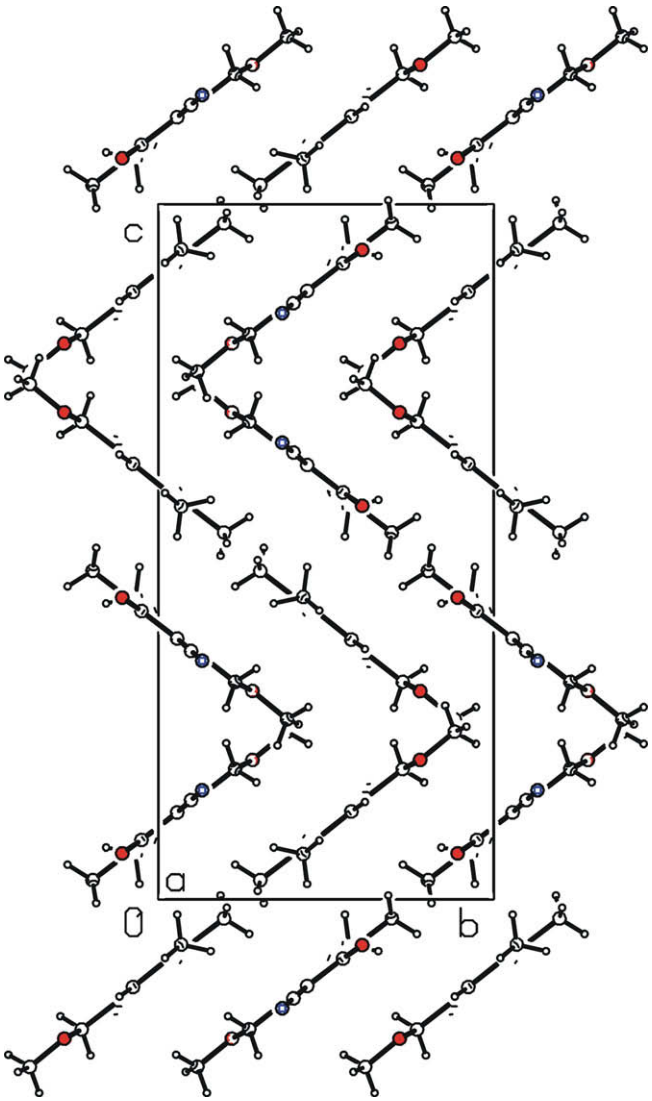

Fig. 4. A crystal packing diagram of **3a**, viewed along the *a* axis, showing the molecules disposed in a herringbone fashion.

200–600 nm. The effects of substituents on the absorption and fluorescence spectra of these compounds are interpreted. Keto-enol tautomerism of compounds **1** and **2** (2-pyridone/2-hydroxypiridine) was investigated by means of electronic spectra and the effects of substituents and solvents.

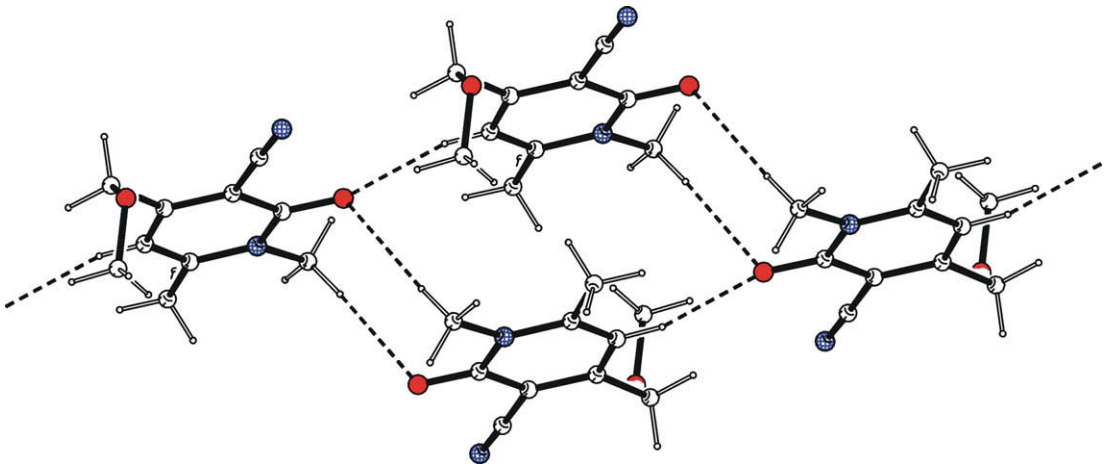

Fig. 5. Part of the crystal structure of **3b**, showing the C–H···O hydrogen bonds which link A independent molecules into infinite chains of tetramers. Hydrogen bonds are indicated by dashed lines.

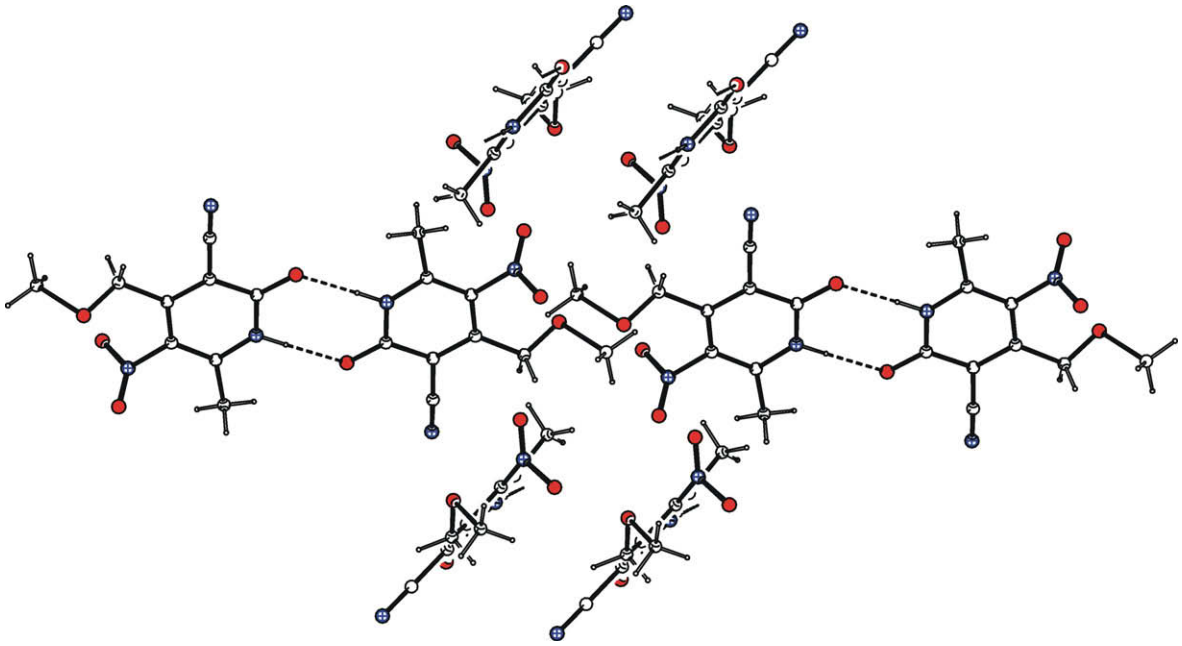

Fig. 6. Part of the crystal structure of **2**, showing centrosymmetric dimers formed by a pairs of self-complementary N1···O1 hydrogen bond. Hydrogen bonds are indicated by dashed lines.

The UV absorption spectra of compounds **1–3** (Fig. 7) contain two maximum absorptions at 224–225 and around 330 nm (λ_{max} (**1**) = 329 nm, λ_{max} (**2**) = 331 nm and λ_{max} (**3**) = 332 nm). That an absorption maxima is in connection with the $\pi \rightarrow \pi^*$ transition of the pyridine ring, and are in agreement with literature data [37].

The fluorescence emission spectra peaks are around 390 nm (λ_{max} (**1**) = 390 nm, λ_{max} (**2**) = 389 nm and λ_{max} (**3**) = 393 nm), for **1**, **2** and **3**, respectively, and they are red-shifted with respect to the absorption spectra. The fluorescence behaviour of compounds **1–3** versus the concentrations in water are shown in Figs. 8–11. For very low concentrations, all of them obey Lambert–Beer's low and the emission intensity increases linearly with increase of concentration. Deviations from Lambert–Beer's low are noticed for concentrations higher than $\approx 10^{-5}$ mol dm^{-3} (Figs. 8 and 11).

The substituent effects of the electron-donating methyl group (compound **3**), which increase the electron density by releasing electrons into a reaction centre, on the absorption and fluorescent spectra affects their absorption and emission spectra, producing a negligible bathochromic shift which depends on their electron-donating ability for only $\Delta\lambda_{max.} = 4$ nm. The effect of electron-donating methyl group can be observed in decreased intensity termed hypochromism ($\Delta\varepsilon_{max} = -7.72 \times 10^6$ dm^3 mol^{-1} cm^{-1}), which is in agreement with literature data that the number and intensity of UV absorption bands are dependent on the conjugation degree between π electrons of heterocycle and the lone electron pair of the substituent [37].

Electron-withdrawing substituent ($-NO_2$) have no significant effect on the position of emission band of compound **2**, hypsochromically shifting the maximum of the UV absorption bands for only $\Delta\lambda_{max} = 1$ nm, but their effect are observed making intensive hypochromic effect which results in decreased emission intensity ($\Delta\varepsilon_{max} = -10.416 \times 106$ dm^3 mol^{-1} cm^{-1}). The decrease in the molar absorptivity (ε) observed here can be related to the effect of the overlap of the orbitals involved in the electronic excitation. Excitation of one electron from the lone par present on the heteroatom to an antibonding π^* orbital ($n \rightarrow \pi^*$), so called «forbidden»

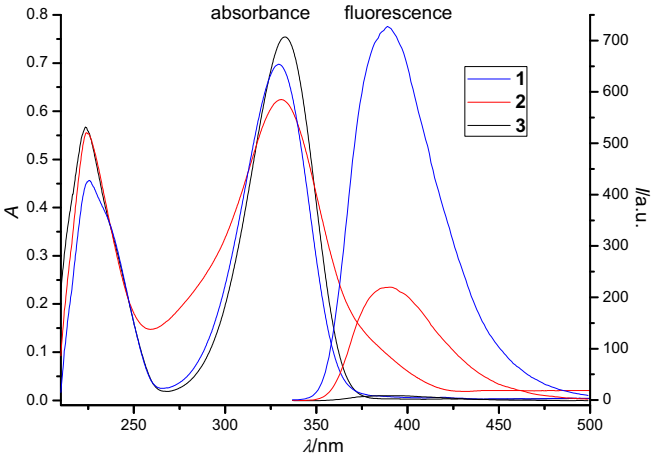

Fig. 7. Absorption spectra and emission spectra of **1**, **2** and **3** in water (c(**1**) = c(**2**) = c(**3**) = 6.5 × 10^{-5} mol dm^{-3}).

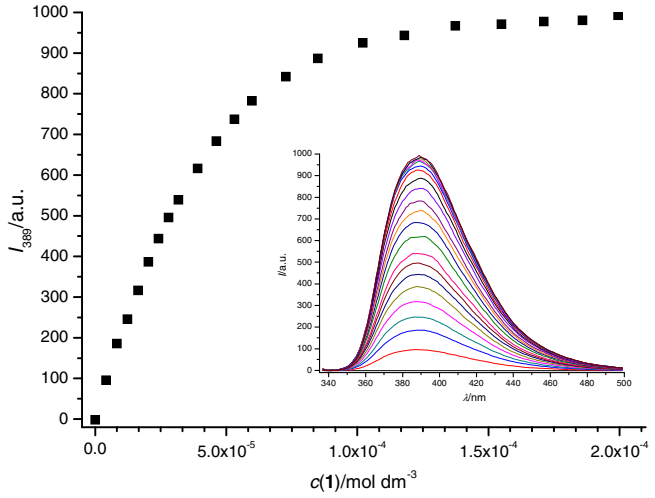

Fig. 8. Emission spectra of **1** in water, intensity as a function of concentration at 25 ± 0.1 °C.

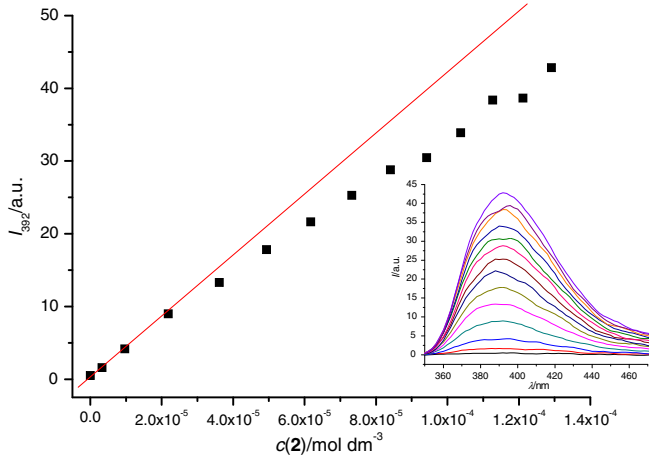

Fig. 9. Emission spectra of **2** in water, intensity as a function of concentration at 25 ± 0.1 °C.

transition is lower in energy than the π → π* «allowed» transition, but the molar absorptivity of the «forbidden» transition is a thousand times smaller than «allowed» transition [38].

The ultraviolet emission wavelength of the electronic transitions of the compounds **1**–**3** in two protic and two aprotic solvents are given in Table 3, and representative spectra are shown in Figs. 12–14.

The emission spectra of compounds **1**–**3** in EtOH, THF and 1,2–dichlorethane is little bathochromically shifted with respect to the emission spectra in water. It was also observed that the emission spectra of all compound **1** in aprotic solvents hypsochromically shifted with respect to the absorption spectra in ethanol. Furthermore, a minor shoulder emission located at around 380 nm was observed for compound **3** in both aprotic solvents (Fig. 14). This phenomenon may be ascribed to the twisted intra molecular charge-transfer reactions [39]. It has been reported that aromatic molecules having the electron-donating group at the para position of an electron-accepting group give fluorescence emission from twisted intra molecular charge-transfer states as well as from the locally excited singlet-transfer in polar and/or non polar solvents. In water, ethanol, tetrahydrofuran, and 1, 2-dichlorethane the sole band appeared at about 380–400 nm ascribable to the 2-pyridone form for compounds **1** and **2**. The emission band at about 400–450 nm due to the 2-hydroxy pyridine form is absent in these spectra [40].

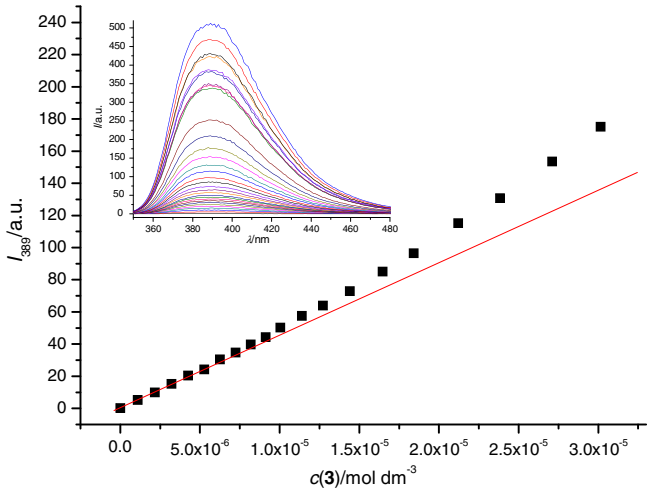

Fig. 10. Emission spectra of **3** in water, intensity as a function of concentration at 25 ± 0.1 °C.

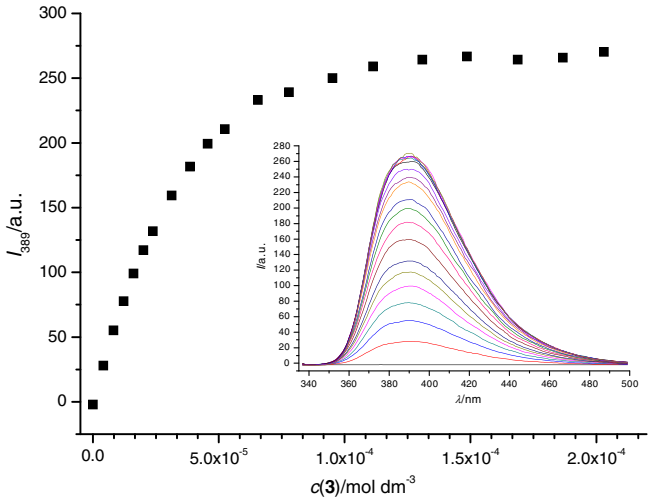

Fig. 11. Emission spectra of **3** in water, intensity as a function of concentration at 25 ± 0.1 °C.

Table 3
Fluorescence data of **1**–**3** recorded in protic and aprotic solvents at the concentration of c(**1**) = c(**2**) = c(3) = 6.5 × 10−5 mol dm^{-3} at 25 ± 0.1 C.

Solvent	λ_{max}/nm			ε_{max}/10^6 dm^3 mol^{-1} cm^{-1}		
	1	**2**	**3**	**1**	**2**	**3**
Water	390	389	393	11.1	0.684	3.38
Ethanol	398	398	395	7.95	0.511	2.42
Tetrahydrofuran	396	398	395	4.60	0.289	1.40
1,2-dichlorethane	395	397	396	2.86	0.165	0.877

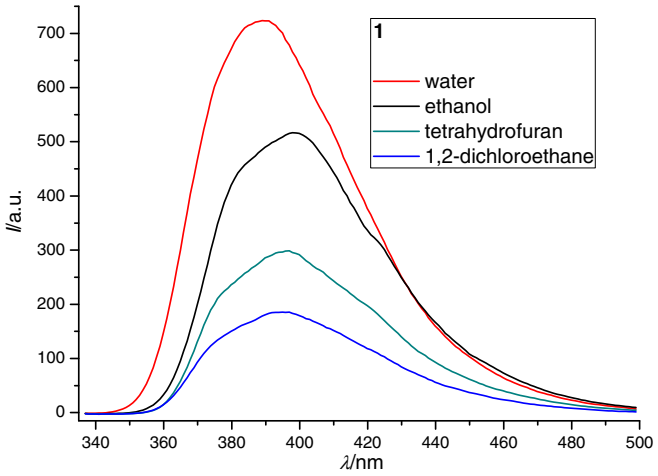

Fig. 12. Fluorescence spectra of **1** in protic and aprotic solvents at 25 ± 0.1 °C (c (**1**) = 6.5 × 10^{-5} mol dm^{-3}).

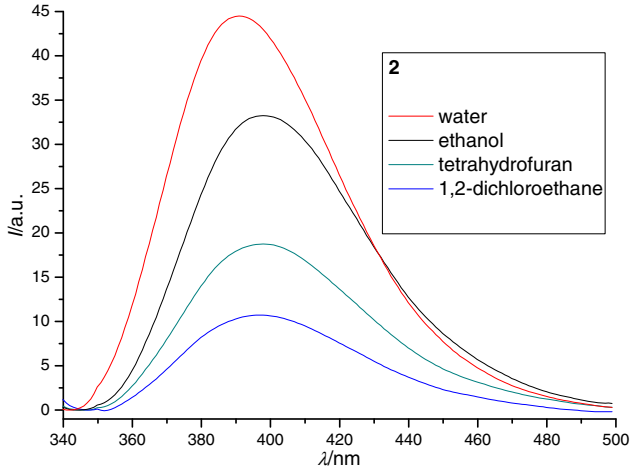

Fig. 13. Fluorescence spectra of **2** in protic and aprotic solvents at 25 ± 0.1 °C (c (**2**) = 6.5 × 10^{-5} mol dm^{-3}).

Solvatochromism of the absorption (λ_{max}, ε) is generally negligible, the emission is more sensitive towards changes of the environment, decreasing polarity causes hypochromic shifts for all compounds ($\Delta\varepsilon_{max}$ = 0.403–8.24 × 10^6 dm^3 mol^{-1} cm^{-1}) and the fluorescence efficiencies are reduced.

3.2.2. IR absorption spectra

The compounds **1** and **2**, prepared in this work, may exist in two tautomeric forms. In the infrared spectra (in KBr) of these compounds the band corresponding to the OH group vibrations in the region 3400–3550 cm^{-1} is absent.

The medium to strong bands observed in the regions 3300 and 3150 cm^{-1} in the IR spectra are assignable to the imino group

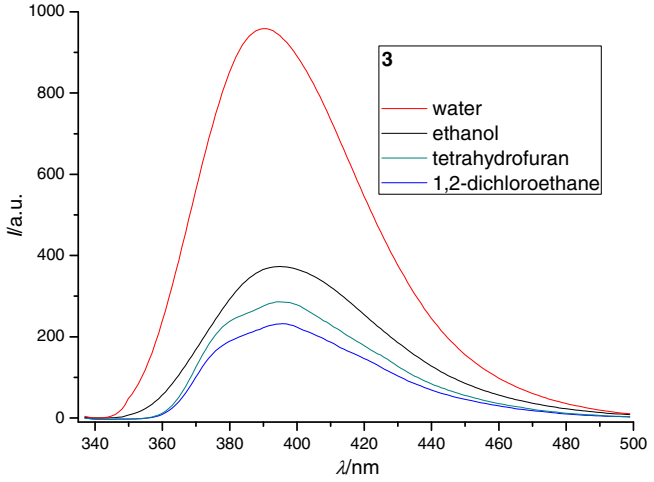

Fig. 14. Fluorescence spectra of **3** in protic and aprotic solvents at 25 ± 0.1 °C(c (**3**) = 6.5 × 10^{-5} mol dm^{-3}).

ν(N—H) stretching band of the ring. The assignment of in-plane d (NH) vibration is very difficult because of the presence of aromatic ring vibrations in this region [41]. So, the medium band observed in the IR spectrum of compounds **1** and **2** at 3312–3302 cm^{-1}, is assigned to the ν(N—H) stretching band of the ring. The other values of bands at 3099–3054 cm^{-1} (aromatic C—H), 3004–2839 cm^{-1} (aliphatic C—H), and 2222–2214 cm^{-1} (C≡N) were also recorded.

The presence of the band at 1658 and 1654 cm^{-1} which is assigned to stretching vibrations ν(C = O) of ring is observed for all compounds, the same like the band at 1584–1578 cm^{-1} assigned to ν(N—H) bending vibration of ring. IR spectrum of the compounds **1** and **2** suggest that these compounds predominantly exist in the 2-pyridone tautomeric form in the solid state.

The IR spectra of compounds **1** and **2** showed strong bands at 1194, 1183 and 573, 568 cm^{-1}, which are attributed to the vibrations of the ν(CONH–) amide bonds. The amide is almost caused by the ν(N–H) stretching vibration [42, 43].

Compound **3** is *N*-methyl derivative, which cannot tautomerize to a pyridine derivative. The IR spectra of the *N*-methyl derivative **3** contained an intense absorption band at 1654 cm^{-1} which belongs to (CO—N–), indicative of the pyridone structure. This observation also shows that the molecules are in keto form, and are in agreement with results of X-ray structure analysis.

Thus, the IR spectrum showed the absence of ν(N—H) stretching and the presence of a band at 3662 cm^{-1} for the (*N*–alkyl) group.

In the IR spectra of the compounds studied the band due to the skeleton deformation of stretching modes pyridine ν(C = C) and ν(C = N) bands in the region 1600–1500 cm^{-1} are not shifted appreciably. In this region interesting features are observed for the (−NO$_2$) symmetric stretch of compound **2**. The −(−NO$_2$) symmetric stretching mode is split into a doublet (1367 cm^{-1}) due to the existence of non-equivalent molecules in the unit cell. In principle, the (−NO$_2$) band should be split into three components. These values are in accordance with the literature [44,45].

The spectral data generally lead to the conclusion that the tautomeric equilibrium of the keto and enol form is in favour of the pyrone form in the solid state.

3.2.3. NMR spectra

The ^{1}H NMR spectra of all investigated compounds measured in DMSO-d$_6$ at 25 °C show a singlet in the range of 2.52–2.47 ppm corresponding to methyl groups (C–6) 3H protons. Multiplets appearing at 3.39–3.36 ppm account for protons due to methoxy groups –O–CH$_3$ (C–4) downfield resonating D$_2$O exchangeable signal integrating for three protons, respectively. Similarly, two

singlets at 4.58 and 4.43 ppm are attributed to two methylene protons of $-CH_2-O-CH_3$ group for all the compounds, respectively.

For compounds **1** and **2** the ^1H NMR spectra exhibit a deuterium oxide exchangeable broad singlet corresponding to OH or NH protons in the region 13.27–12.49 ppm, and for compounds **1** and **3** a signal in the range of 6.28–6.42 is assigned to the H-5 proton.

The ^1H NMR spectrum of compound **3** showed signals from the starting pyridone **1,** and the absence of the broad singlet signal approximately at 13 ppm corresponding to OH or NH protons. The disappearance of these signals indicates that compounds **1** and **2** exist exclusively as 2(1H) pyridone tautomers.

The structures of the title compounds are further substantiated by the ^{13}C APT-NMR, spectroscopic data measured in DMSO-d_6. The spectroscopic data of compounds **1**–**3** indicate that the carbons atoms give rise to different peaks within the frequency range of 17.70–160.84 ppm. The quaternary carbons signals in the 159.41–160.93 ppm regions are assignable to CO of the CO–NH amide group. Quaternary carbons is observed in the ^{13}C APT-NMR of all compounds at 160.19–151.26 ppm (C–4), at 155.16–152.21 ppm (C–3), 114.21–115.60 ppm (C–6) and at 101.56–96.25 ppm (C≡N), respectively.

Singlets are observed for secondary methylene carbons of $—CH_2—O—CH_3$ group of all compounds at 70.80–69.73 ppm. Similarly, two singlets at 59.26–58.89 and 17.70–21.56 ppm, respectively are attributed to primary carbons of methyl group.

As expected, significant changes are observed for chemical shift values of primary carbon of methyl group which appeared approximately at 31.83 ppm, only for compound **3**, compared with the starting material.

In the spectrum of compound **2**, the shift of the C-5 peak to the downfield region at 151.82 ppm of tertiary carbons supports with the formation of $-NO_2$ group, and thus confirms nitration process.

The results inferred from the IR and NMR spectral data of compounds **1**–**3** are found to be in agreement with the proposed structure which were supported by X-ray diffraction data.

4. Conclusions

Three substituted 2-pyridones (**1**–**3**) were synthesized by modified procedure and corresponding molecular structure was experimentally characterized by means of IR and UV–vis spectroscopy techniques. The structures of compounds **2** and **3** were confirmed by single crystal X-ray diffraction method. On the basis of X-ray and IR spectroscopic data have been determined that compounds **1** and **2** are in keto form in the solid state. UV–vis spectra of compounds **1**–**3** were recorded in protic and aprotic solvents. In the fluorescent spectra of compounds **2** and **3** were found hypochromic effect which exhibits a strong solvent dependence. This effect can be from «forbidden» transitions which are related to the effect of the overlap of the orbital involved in the electronic excitation. X-ray crystal structure analysis shows that molecules of **2** are linked by one N–H···O hydrogen bond into dimers. The molecules of orthorhombic polymorph of **3** are held together only by van der Waals forces. In supramolecular aggregation of its triclinic polymorph participates two C–H···O hydrogen bonds which form chain of tetramers.

Acknowledgements

Support for this study by the Ministry of Science and Technology of Croatia (project No. 058-2261-2253 and 119-1193079-3069) is gratefully acknowledged.

Appendix A. Supplementary data

Supplementary data associated with this article can be found, in the online version, at doi:10.1016/j.molstruc.2010.01.038.

References

[1] P.S. Dragovich, T.J. Prins, R. Zhou, E.L. Brown, F.C. Maldonado, S.A. Fuhrman, L.S. Zalman, T. Tuntland, C.A. Lee, A.K. Patick, D.A. Matthews, T.F. Hendrickson, M.B. Kosa, B. Liu, M.R. Batugo, J.-P.R. Gleeson, S.K. Sakata, L. Chen, M.C. Guzman, J.W. Meador, R.A. Ferre, S.T. Worland, J. Med. Chem. 45 (2002) 1607.
[2] Q. Li, L.A. Mitscher, L.L. Shen, Med. Res. Rev. 20 (2000) 231.
[3] R.J. Cox, D.J. O'Hagan, Chem. Soc. Perkin Trans. 1 (1991) 2537.
[4] P.S. Dragovich, T.J. Prins, R. Zhou, T.O. Johnson, E.L. Brown, F.C. Maldonado, S.A. Fuhrman, L.S. Zalman, A.K. Patick, D.A. Matthews, X. Hou, J.W. Meador, R.A. Ferre, S.T. Worland, Bioorg. Med. Chem. Lett. 12 (2002) 733.
[5] W.K. Anderson, D.C. Dean, T.J. Endo, Med. Chem. 33 (1990) 1667.
[6] J.N. Heo, Y.S. Song, B.T. Kim, Tetrahedron Lett. 46 (2005) 4621.
[7] D.L. Comins, J.M. Nolan, Org. Lett. 3 (2001) 4255.
[8] R.K. Beckman, J.C. Potenza, E.J. Enholm, J. Org. Chem. 52 (1987) 469.
[9] E.L. Presti, R. Boggia, A. Feltrin, G. Menozzi, P. Dorigo, L. Mosti Farmaco 54 (1999) 465.
[10] P. Dorigo, D. Fraccarolo, R.M. Gaion, G. Santostasi, P.A. Borea, M. Floreani, L. Mosti, I. Maragno, Gen. Pharm. 28 (1997) 781.
[11] C. Altomare, S. Cellamare, L. Summo, P. Fossa, L. Mosti, A. Carotti, Bioorg. Med. Chem. 8 (2000) 909.
[12] E. De Clercq, Il Farmaco 54 (1999) 26.
[13] R.L.T. Parreira, O. Abrahao, S.E. Galembeck, Tetrahedron 57 (2001) 3243.
[14] P. Deshang, J.A. Cipollina, N.K. Lowmoster, J. Org. Chem. 53 (1988) 1356.
[15] K. Seibold, G. Wagniere, H. Labhard, Helv. Chim. Acta 52 (1969) 789.
[16] D.L. Comins, J.K. Saha, J. Org. Chem. 61 (1996) 9623.
[17] F.A. Cotton, R.A. Walton, Multiple Bonds between Metal Atoms, second ed., Clarendon Press, Oxford, 1993.
[18] O. Kahn, Molecular Magnetism, VCH, New York, 1993.
[19] E. Coronado (Ed.), Molecular Magnetism: from Molecular Assemblies to the Devices, Kluwer Academic, Dordrecht, 1996.
[20] T. Mochida, M. Ueda, C. Aoki, H. Mori, Inorg. Chim. Acta 335 (2002) 151.
[21] M. Jukić, M. Cetina, G. Pavlović, V. Rapić, Struct. Chem. 10 (1999) 85.
[22] M. Jukić, A. Hergold-Brundić, M. Cetina, A. Nagl, J. Vorkapić-Furač, Struct. Chem. 14 (2003) 597.
[23] M. Jukić, M. Cetina, J. Vorkapić–Furač, A. Golobić, A. Nagl, Acta Crystallogr. C59 (2003) 357.
[24] Oxford Diffraction, Xcalibur CCD System. *CrysAlis CCD* and *CrysAlis RED*. Oxford Diffraction Ltd., Abingdon, England.
[25] G.M. Sheldrick, Acta Crystallogr. A64 (2008) 112.
[26] A.L. Spek, J. Appl. Crystallogr. 36 (2003) 7.
[27] (a) W.F. Bruce, H.W. Coover, J. Am. Chem. Soc. 66 (1944) 2092;
(b) W. Werner, J.T. Plati, J. Org. Chem. 11 (1946) 751;
(c) A.S. Harris, K. Folkers, J. Am. Chem. Soc. 61 (1939) 1245.
[28] D. Conreaux, E. Bossharth, N. Monteiro, P. Desbordes, G. Balme, Tetrahedron Lett. 46 (2005) 7917.
[29] F.H. Allen, Acta Crystallogr. B58 (2002) 380. Version 5.30, September 2009.
[30] V.B. Rybakov, A.A. Bush, E.V. Babaev, L.A. Aslanov, Acta Crystallogr. E60 (2004) o160.
[31] D.V. Albov, E.I. Turubanova, V.B. Rybakov, E.V. Babaev, L.A. Aslanov, Acta Crystallogr. E60 (2004) o1222.
[32] Y.C. Wang, X.S. Wang, Z.S. Zeng, D.Q. Shi, Acta Crystallogr. E61 (2005) o3261.
[33] A. Basheer, Z. Rappoport, J. Org. Chem. 73 (2008) 1386.
[34] P. Valerga, M.C. Puerta, Private Communication (2007) (CSD code XIMSOC).
[35] P. Valerga, M.C. Puerta, Private Communication (2007) (CSD Code XIMTOD).
[36] J. Bernstein, R.E. Davis, L. Shimoni, N.L. Chang, Angew. Chem. Int. Ed. Engl. 34 (1995) 1555.
[37] G.G. Beamish, Practical Fluorescence, second ed., Marcel Dekker, New York, 1990.
[38] P.S. Kalsi, Spectroscopy of Organic Compounds, sixth ed., New Age International Publishers, New Delhi, 2007. p. 16.
[39] L.D.S. Yadav, Organic Spectroscopy, Kulver Academic Publishers, Dorderecht, The Netherlands, 2005. p. 42.
[40] C. Reichardt, Solvents and Solvent Effects in Organic Chemistry, John Wiley, Weinheim, 2004, p. 113.
[41] N.M. Aghatabay, Y. Mahmiani, H. Cevik, F. Gucin, B. Dulger, Struct. Chem. 19 (2008) 833.
[42] H. Gűnzer, H.U. Gremlich, IR Spectroscopy: An Introduction, Wiley-VCH Verlag GmbH, Weinheim, 2002. pp 224–226.
[43] S. Chandra, L.K. Gupta, Spectrochim. Acta A Mol. Biomol. Spectrosc. 62 (2005) 1102–1106.
[44] J. Hanuza, M. Mączka, A. Waśkowska, W. Oganowski, H. Ban-Oganowska, B. Lutz, J.H. van der Maas, Vib. Spectrosc. 14 (1997) 49.
[45] J. Hanuza, M. Mączka, A. Waśkowska, W. Oganowski, H. Ban-Oganowska, B. Lutz, J.H. van der Maas, J. Mol. Struct. 450 (1998) 201.